ADVANCED OPTICAL MATERIALS
www.advopticalmat.de

Determination of Free Charge Carrier Luminescence and Quasi-Fermi Level Separation in Organic Solar Cells via Transient Photoluminescence Measurements

*Mathias List, Jared Faisst, Friedemann Heinz, and Uli Würfel**

The detection of photoluminescence (PL) is extremely valuable for photovoltaic technologies as it provides direct information about the free charge carrier densities and therefore about the separation of the quasi-Fermi levels (ΔE_F). However, for organic solar cells the PL is strongly dominated by photogenerated excitons that in part decay radiatively before they form free charge carriers via dissociation at a donor/acceptor interface. For this reason, it is impossible to deduce the free charge carrier densities and ΔE_F directly from the PL signal. To overcome this severe limitation, a new approach is developed that allows disentangling the luminescence of photogenerated excitons from the one of free charge carriers. Due to the large difference in respective lifetimes—for photogenerated excitons it is ≤ ns whereas for free charge carriers it is in the µs-range—this is achieved by time-resolved PL measurements. For highly efficient organic solar cells, it is found that ΔE_F determined from these PL transients matches perfectly with the electrical voltage. Moreover, the new method also allows for the determination of ΔE_F from mere absorber films without electrodes and thus paves the way for a better understanding of organic solar cells.

1. Introduction

Organic photovoltaics (OPV) does neither rely on any critical elements such as heavy metals or rare earth elements nor does it require the use of higher temperatures, thus rendering it a PV technology that could be produced with minimized environmental impact. Attractive features are moreover their light weight and flexibility as well as their homogeneous appearance on large areas including a tunable visible transparency. The efficiency of small area champion devices could be brought up significantly in the last few years to values beyond 19%.[1–5] Nevertheless, considerable challenges for future commercialization of OPV devices remain. This includes the transfer of these high efficiencies to large-area, long-term stable modules. Future improvements in the performance of OPV devices can be achieved by novel photoactive materials capable of harvesting a larger part of the solar spectrum. Energy alignment between donor and acceptor of the photoactive layer as well as at the interfaces between the absorber layer and the electron and hole transport layers also plays a crucial role to realize efficient charge generation as well as selective charge carrier extraction and thus high voltages. For a knowledge-based optimization of PV devices profound data is needed that is gained by the application of different characterization techniques. Among them, the detection of photo- and electroluminescence (of free charge carriers) proved to be very useful as it provides direct information about the optoelectronic properties of the device. These techniques have gained significant importance in the characterization of solar cells and modules as they are non-destructive and fast that allows using them in, e.g., an in-line inspection in a manufacturing line. Moreover, from the measurement result, i.e., the luminescence intensity of free charge carriers, the internal separation of the quasi-Fermi levels ΔE_F can be derived.[6–25] Especially photoluminescence (PL) is very interesting for the following two reasons. First, PL allows insight into the recombination of photogenerated charge carriers under real operation conditions in contrast to electroluminescence (EL) where recombination of electrically injected charge carriers is investigated in the dark. Second, since the charge carriers are generated by absorption of light PL can already be applied at a pre-stage of cell or module manufacturing as no electrodes are required.

M. List, J. Faisst, F. Heinz, U. Würfel
Fraunhofer Institute for Solar Energy Systems ISE
Heidenhofstr. 2, 79110 Freiburg, Germany
E-mail: uli.wuerfel@ise.fraunhofer.de
U. Würfel
Freiburg Materials Research Center FMF
University of Freiburg
Stefan-Meier-Str. 21, 79104 Freiburg, Germany

The ORCID identification number(s) for the author(s) of this article can be found under https://doi.org/10.1002/adom.202300895

DOI: 10.1002/adom.202300895

2. Results and Discussion

2.1. Luminescence in OPV

Investigating the PL of free charge carriers in organic photovoltaic devices is however by far not as straightforward as in the

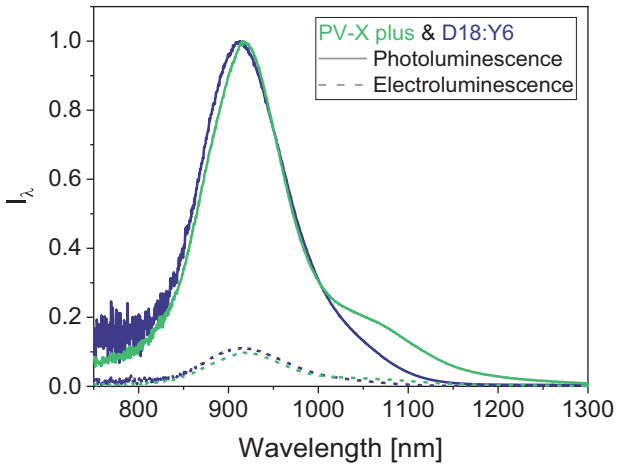

Figure 1. Photo- and electroluminescence spectra of a D18:Y6 and a PV-X plus solar cell. The PL spectra (solid lines) are normalized and the corresponding EL spectra (dashed lines) are scaled accordingly. All spectra are corrected for the optical outcoupling efficiency of the respective layer stack, see text.

case of crystalline inorganic semiconductors. This is due to the presence of various emissive species in the more complex generation and recombination processes occurring in organic solar cells. In an organic absorber layer comprising a donor:acceptor system the absorption of photons generates local excitons (LE) in the donor and/or acceptor phase that typically do hardly dissociate into free charge carriers in the pristine phases due to their rather strong coulombic binding energy.[26–30] Such an LE will therefore either recombine (partly radiatively) or it is dissociated at the donor:acceptor interface and thus forms a pair of free charge carriers, a free electron in the acceptor and a free hole in the donor. The latter is often referred to as charge separated state in the context of OPV. The free charge carriers can then either be extracted at the contacts and thus contribute to the external electrical current or they recombine (again to some extent radiatively) inside the photoactive material at a donor:acceptor interface. Since both photogenerated local excitons and free charge carriers can decay in a radiative manner the photoluminescence of an OPV device is the superposition of these two processes. Although discussed further below we want to stress already here that free charge carriers in an organic solar cell do not recombine directly, but rather through so called charge transfer (CT) states at the donor:acceptor interface or even by forming secondary LE.

For this study, two high-efficiency organic absorber materials are investigated, D18:Y6 and PV-X plus delivering power conversion efficiencies of 15.7% and 15.5%, respectively. For better readability, the short names for the absorber materials are used here. The long chemical names, cell stacks, and processing parameters are listed in the section "Solar Cell Preparation", corresponding current–voltage (*J*–*V*) curves can be found in the Supporting Information.

The normalized PL spectra (spectral energy density) of the two different OPV devices under an illumination equivalent to "1 sun" (AM1.5G, corrected for spectral mismatch) are depicted in **Figure 1** together with the EL spectra that are rescaled by the very same factor used for the normalization of the corresponding PL spectra. For the EL measurements, injection currents equivalent to the respective photogenerated currents related to the PL measurements were applied. The spectra are corrected for the optical outcoupling efficiency[31] of the layer stack as described in the Supporting Information in detail.

During an EL experiment, free charge carriers are injected through the electrodes that then recombine with each other within the absorber layer. In contrast to a PL experiment, no photogenerated LE are present in the case of EL as it is measured in the dark. Therefore, the EL signal provides a reasonable estimate of the share of the free charge carrier luminescence within the total PL signal when ensuring an equivalent (recombination) current to be injected (EL) as is photogenerated under illumination (PL). Under illumination, it can be seen that the expected free charge carrier luminescence is typically obscured by the strong luminescence of photogenerated LE. It is worth noting here that in the presented D18:Y6 high-efficiency organic absorber material ≈99% of the photogenerated excitons actually do generate free charge carriers and only ≈1% recombine (and a fraction thereof radiatively).[32] Since all free charge carriers have to recombine under open-circuit conditions the free charge carrier recombination current exceeds the exciton recombination current by about two orders of magnitude. Nevertheless, Figure 1 shows that the free charge carrier luminescence (EL) is an order of magnitude lower than the PL that is strongly dominated by the small fraction of LE that recombine radiatively. From these two ratios—1% of the photogenerated LE generate a luminescence that is ten times as strong as the free charge carriers for the same recombination current—we can estimate that the probability of the recombination of photogenerated LE to be radiative is higher by a factor of $\approx 10^3$ compared to the one of free charge carriers.

The challenge to be overcome here is that the large PL contribution of the photogenerated LE and therefore also the overall PL signal does not scale with the concentration of free charge carriers and thus also not exponentially with the quasi-Fermi level separation. Hence, in order to nevertheless derive ΔE_F from the PL signal, the latter must be separated into the part stemming from the radiative decay of photogenerated LE and the part originating from the radiative recombination of free charge carriers. Different efforts to achieve this goal were reported in the literature. Spies et al. have used the difference in steady-state PL intensities at different working conditions to estimate the free charge carrier luminescence.[33] Riley et al. have used a combination of PL and EL to determine the steady-state ΔE_F.[34] Further, Phuong et al. used photoinduced absorption to quantify the photogenerated concentration of holes under different illumination intensities and thus determine the steady-state ΔE_F.[35]

In this work, we present a novel, completely different approach to identifying the contribution of free charge carriers to the overall photoluminescence. As a matter of fact, regardless of the spectral overlap of the luminescence of photogenerated local excitons and free charge carriers their respective lifetimes differ strongly from each other. Common lifetimes of local excitons (τ_{LE}) in OPV materials were determined to be in the sub-nano to nanosecond range.[36–40] In contrast, free charge carrier lifetimes (τ_{free}) have been reported to be in the µs-range at relevant illumination intensities.[41–44] Moreover, this was also confirmed for the materials used in this study by the transient EL method presented in our previous work.[45]

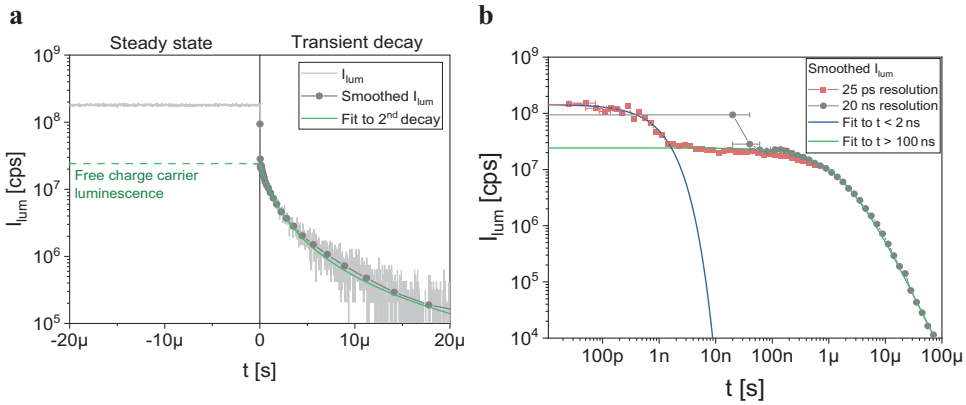

Figure 2. Transient PL of a PV-X plus OPV device. PL intensity I_{lum} (light grey line) and the smoothed data (dark grey line with symbols) over time a) showing a constant steady-state PL during illumination ($t < 0$) followed by a rapid initial decay and a second slower decay. The transient PL is visualized in a double logarithmic plot (b). Here, a measurement with a resolution of 25 ps (red line with symbols) is added that resolves the fast decay of photogenerated excitons (limited by the fall time of the illumination, see text) fitted with an exponential decay (blue). The lower time resolution of 20 ns resolves the second decay over a longer time span, revealing the decay of free charge carriers that is fitted for $t > 100$ ns (green). The corresponding amplitude (at $t = 0$) resembles the steady-state free charge carrier luminescence (dashed green line) as also depicted in (a).

Thus, in order to obtain the PL of free charge carriers directly—to the best of our knowledge for the first time—we make use of these vastly different lifetimes of photogenerated local excitons and free charge carriers. To do so, we detect the time-resolved PL intensity before (i.e., in the steady-state) and after a fast switch-off of the light source.

2.2. Transient Photoluminescence

In the transient PL measurements presented in this work the device is illuminated with a constant intensity until steady-state conditions are established resulting in the respective steady-state LE and free charge carrier densities $n_{LE,0}$ and $n_{free,0}$. Thereafter the illumination is switched off (at $t = 0$). The time-resolved radiative recombination R_{rad} can therefore be described by

$$R_{rad}(t) = \begin{cases} R_{rad,LE}(n_{LE,0}) + R_{rad,free}(n_{free,0}) & \text{for } t \le 0 \\ R_{rad,LE}(n_{LE}(t)) + R_{rad,free}(n_{free}(t)) & \text{for } t > 0 \end{cases} \quad (1)$$

The rate of radiative LE recombination as a function of the LE density n_{LE} is denoted as $R_{rad,LE}(n_{LE})$. Accordingly, $R_{rad,free}(n_{free})$ is the rate of radiative free charge carrier recombination. Within a few nanoseconds after the illumination is turned off (i.e., $t \gg \tau_{LE}$) the observed PL can be expected to consist predominantly of the remaining free charge carrier luminescence while the photogenerated local excitons and therewith their luminescence has already vanished.

$$R_{rad}(t) \approx R_{rad,free}(n_{free}(t)) \quad \text{for } t \gg \tau_{LE} \quad (2)$$

For the experiment it is important to note that the detected PL intensity (I_{lum} [s^{-1}]) is proportional to the volume integral of the radiative recombination rate R_{rad}

$$I_{lum} = \frac{\Omega}{4\pi}\, \alpha\, A \int_0^d R_{rad}(x)\, dx = \frac{\Omega}{4\pi}\, \alpha\, A\, d\, R_{rad} \quad (3)$$

Here, spatially homogeneous recombination within the photoactive layer of thickness d is assumed, A is the area observed, Ω is the solid angle of acceptance of the detector and α is a material and layer stack specific efficiency of detection that is independent of the illumination intensity. It accounts for the spectral shape of emission, the outcoupling efficiency of light from the specific layer stack and the efficiency of the detector (the formula and a detailed derivation of α is given in the Supporting Information).

Figure 2a depicts the transient PL intensity $I_{lum}(t)$ of a PV-X plus cell. Under steady-state conditions ($t \le 0$) the cell is illuminated with a constant laser intensity such that the short-circuit current density J_{SC} equals the one measured under "1 sun" (simulated AM1.5G, corrected for spectral mismatch). The luminescence (light grey) is acquired using a 20 ns time binning. In addition, the smoothed intensity (dark grey) using logarithmic time binning (described in the Supporting Information) is shown as line with symbols. The latter is plotted on a logarithmic time scale (Figure 2b) to better visualize the entire decay. For higher temporal resolution at the beginning, a measurement with a 25 ps bin size (red) is included. Here, both detected luminescence intensities are plotted as lines with symbols including their according bin size as temporal error bars. The initial decay with short lifetime is fitted for $t < 2$ns with an exponential decay (blue). This rapid decay of photogenerated exciton luminescence follows the fall time of the laser that is ≈1 ns (see Supporting Information), thus not allowing to resolve the LE lifetime. Thereafter, the remaining luminescence decay, i.e., the radiative decay of free charge carriers is resolved over five orders of magnitude in time and fitted for $t > 100$ ns using a fit function (green) that solves the continuity equation for free charge carriers (the derivation and fit function is given in Equation S3 (Supporting Information). The fit is in excellent agreement with the measured transient PL data over the entire detected range after the rapid initial decay and thus allows the determination of the initial steady-state free charge carrier luminescence $I_{lum}(n_{free,0})$ by extrapolation to $t = 0$. The extrapolated luminescence intensity is about an order of magnitude lower than the steady-state luminescence. Note that

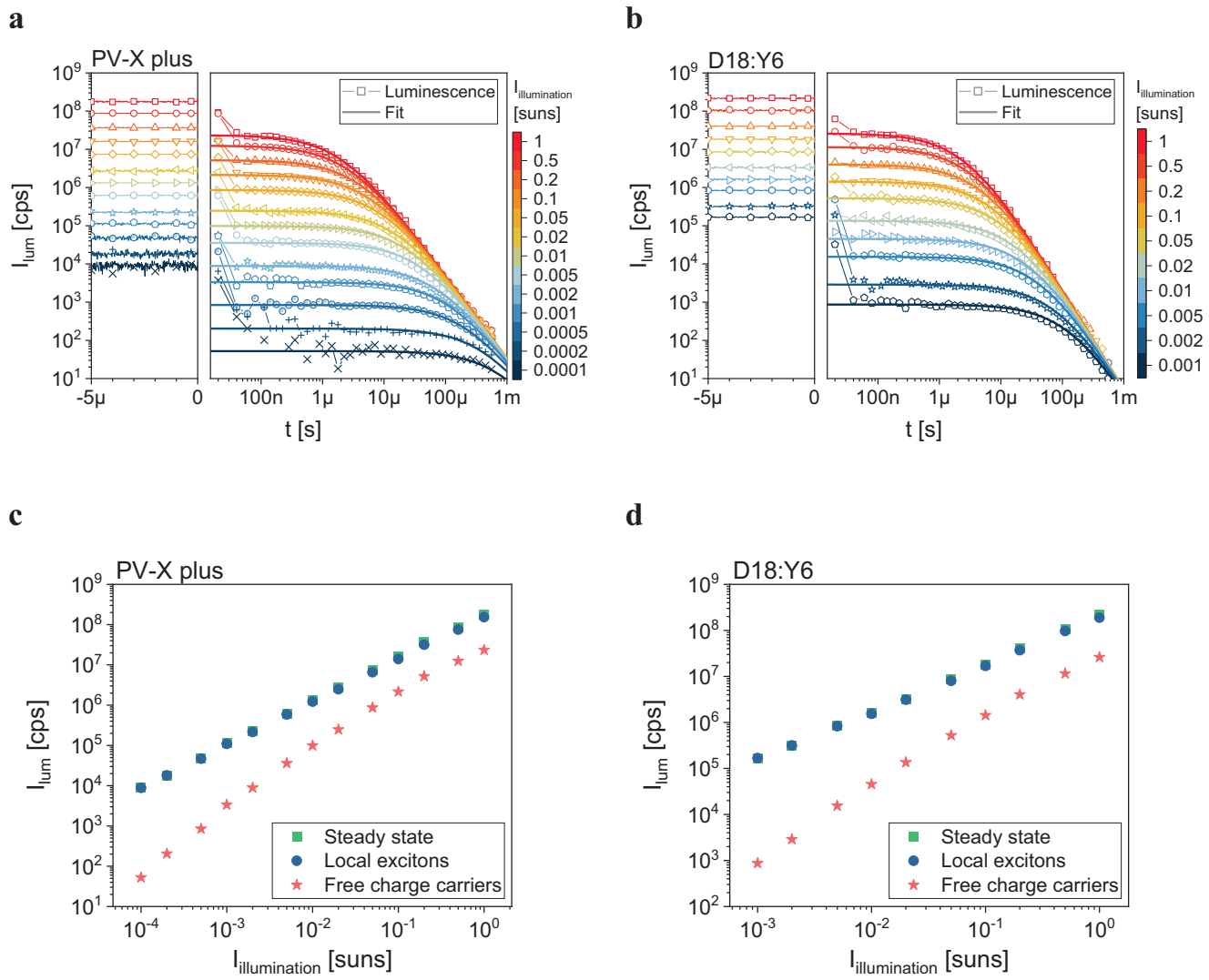

Figure 3. Illumination intensity dependent transient PL of OPV devices and extrapolated local exciton and free charge carrier contributions. The steady-state and transient PL intensity I_{lum} for a) a PV-X plus and b) a D18:Y6 organic solar cell, respectively, for various illumination intensities (thin lines with symbols) alongside the fit functions for the free charge carrier contributions (thick solid lines) for $t > 100$ ns. In (c,d) the total steady-state PL intensities (green squares), the extrapolated ($t = 0$) steady-state free charge carrier luminescence (red stars) and the steady-state local exciton luminescence (blue circles) are plotted over the illumination intensity for the two materials, respectively.

this is also in perfect agreement with the expected range for the share of steady-state free carrier luminescence (EL) within the total signal (PL) as estimated from Figure 1.

In the following, the D18:Y6 and the PV-X plus solar cell are both investigated in more detail using this method. **Figure 3**a,b depicts the transient PL intensities (line with symbols) for different illumination intensities ($I_{illumination}$) in multiples of "1 sun" for both materials. Here, the steady-state signal ($t < 0$) is plotted logarithmically over a linear time scale while the (smoothed) transient decay is plotted double logarithmically. The fit functions (solid lines) to the transient decays for $t > 100$ ns are included as lines. Again, extrapolating these fit functions to $t = 0$ yield the steady-state free charge carrier luminescence $I_{lum}(n_{free,0})$.

Figure 3c,d shows the steady-state luminescence intensities as a function of the illumination intensity. The total steady-state luminescence is plotted (green squares) together with the free charge carrier steady-state luminescence (red stars). The LE steady-state luminescence (blue circles) is given by their difference $I_{lum}(n_{LE,0}) = I_{lum} - I_{lum}(n_{free,0})$. For both material systems it can be observed that the LE luminescence increases nearly linearly with illumination intensity whereas the assigned free charge carrier luminescence does not.

2.3. Photoluminescence and Implied Voltage

The crucial question is whether the extrapolated steady-state luminescence intensities $I_{lum}(n_{free,0})$ given in Figure 3c,d are indeed the proclaimed free charge carrier luminescence intensities and thus proportional to the product of the steady-state free

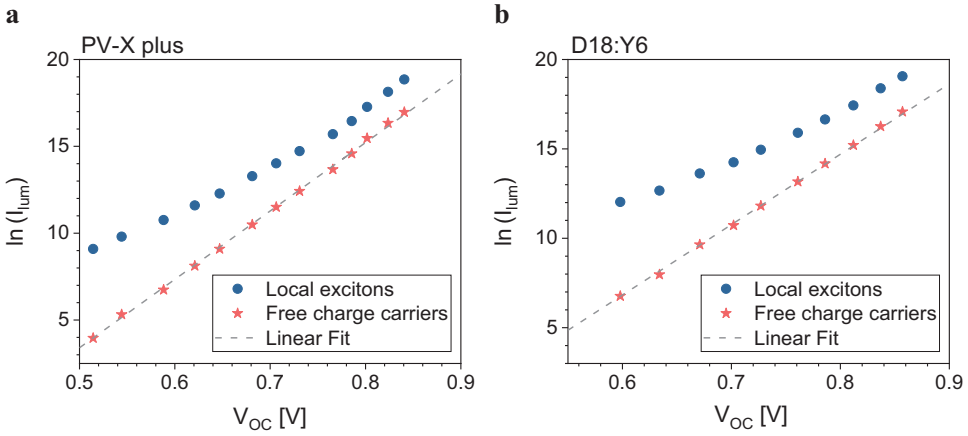

Figure 4. Local exciton and free charge carrier steady-state PL as a function of the open-circuit voltage. The determined local exciton (blue circles) and free charge carrier (red stars) steady-state PL intensities I_{lum} for a) a PV-X plus solar cell and b) a D18:Y6 solar cell versus the open-circuit voltage V_{OC} alongside linear fits (dashed grey lines) to the free charge carrier luminescence according to Equation (6).

charge carrier densities ($n_{e,0}\ n_{h,0} = n^2_{free,0}$) for the corresponding illumination intensities, i.e., whether the following assumption holds true

$$I_{lum}\ \left(n_{free,0}\right) = \frac{\Omega}{4\pi}\ \alpha\ A\ d\ k_{rad,free}\ n^2_{free,0} \tag{4}$$

To validate this, the determined steady-state free charge carrier luminescence intensities are compared to the voltages measured between the electric contacts of the device. Therefore, we introduce first the implied voltage as $V_{imp} = e^{-1}\Delta E_F$, with e being the elementary charge. It is given by

$$V_{imp} = e^{-1}\ \Delta\ E_F = \frac{k_B T}{e}\ \ln\left(\frac{n^2_{free,0}}{n_i^2}\right) \tag{5}$$

with n_i being the intrinsic free charge carrier density. Combining Equations (4) and (5) yields an expected linear correlation between the natural logarithm of the steady-state free charge carrier luminescence and V_{imp} with a predetermined slope of $e/k_B T$ and a (constant) offset $C = \ln(n_i^2 k_{rad,\ free}\frac{\Omega}{4\pi}\alpha A d)$.

$$\ln\ \left(I_{lum}\ \left(n_{free,0}\right)\right) = \frac{e}{k_B T}\ V_{imp} + C \tag{6}$$

For selective contacts (i.e., rendering surface recombination negligible) the steady-state open-circuit voltage of the device (V_{OC}) is assumed to equal the implied voltage ($V_{OC} = V_{imp}$) and Equation (6) should therefore hold true using V_{OC} as well. Note that the advantage of our method is that during the detection of the photoluminescence the voltage between the terminals can be measured simultaneously. Therefore, the natural logarithm of the steady-state luminescence of LE (blue) and free charge carriers (red) is plotted versus V_{OC} for the PV-X plus device (**Figure 4**a) and for the D18:Y6 device (Figure 4b). The data for the free charge carriers is fitted by a linear function according to Equation (6) with slope $e/k_B T$ for a temperature of $T = 293$ K.

It can be seen that the expected linear correlation described by Equation (6) is given for the steady-state free charge carrier luminescence. This shows clearly that the remaining PL after the fast initial photogenerated LE decay indeed originates from the radiative recombination of free charge carriers.

Consequently, the constant offsets can be determined as $C_{D18:\ Y6} = -16.78$ and $C_{PV-X\ plus} = -16.28$ that allows a direct determination of V_{imp} under illumination. In addition, it becomes obvious from Figure 4a,b that the natural logarithm of the steady-state luminescence of photogenerated LE is indeed not proportional to V_{OC} and thus is not proportional to the product of the free electron and hole densities as already assumed above.

Another question is whether the accordance of V_{imp} and V_{OC} also holds during the transient charge carrier decay. It is now straightforward to convert the time-resolved intensity $I_{lum}(n_{free}(t))$ into an implied voltage using Equation (6) and the determined offsets $C_{D18:\ Y6}$ and $C_{PV-X\ plus}$ for the respective materials. The resulting transient $V_{imp}(t)$ is plotted together with the $V_{OC}(t)$ as measured simultaneously between the terminals for the PV-X plus (**Figure 5**a) and for the D18:Y6 solar cell (Figure 5b).

Again, excellent agreement is observed over the entire resolvable decay. This shows clearly that the free charge carrier luminescence is in equilibrium with the product of the free electron density (in the acceptor) and the free hole density (in the donor) and the corresponding implied voltage equals the V_{OC} at the terminals in the transient case as already shown for the steady-state. In general, free charge carriers can decay radiatively on a pair of interacting molecules at the donor:acceptor interface, referred to as charge transfer (CT) state in the field of OPV, or via re-formed secondary LE in a pristine phase in case of strong electronic coupling. Such strong coupling between CT and LE states in the acceptor phase was recently reported for state-of-the-art high efficiency organic solar cells based on donor polymers with non-fullerene acceptors as also used in this study.[25,46,47] This coupling between the CT and LE states is strongly supported by the fact that the observed EL and PL spectra in Figure 1 are of indistinguishable spectral shape. This means that the radiative decay of both free charge carriers and photogenerated LE occurs predominantly over the same LE state. Thus, the presented results imply that radiatively recombining free charge carriers do this by forming secondary LE. Nevertheless, it is important to note that

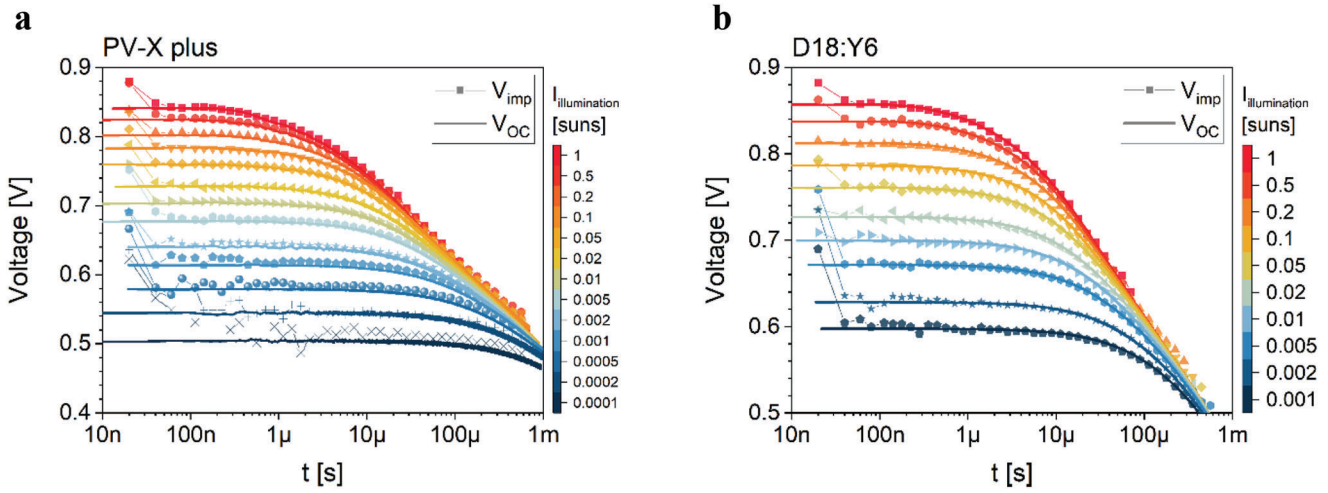

Figure 5. Time-resolved implied voltage and open-circuit voltage. The time dependent implied voltage V_{imp} in the absorber determined from the transient PL intensity using Equation (6) and the open-circuit voltage V_{OC} for a) the PV-X plus and b) the D18:Y6 organic solar cell for various illumination intensities.

this emission is, in contrast to the one of the radiatively decaying photogenerated LE, in equilibrium with the free electron and hole densities in the respective pristine materials. In other words, these LE states (now populated by secondary LE) can be described by the same quasi-Fermi levels as the free charge carriers and thus by V_{imp}. Our findings show clearly that this is the case both for steady-state and transient PL. This is also well in accordance to what was shown for transient EL in our previous work.[45] Note further that the method is not limited to high-efficiency organic solar cells that show the mentioned strong coupling between CT and LE states. It can also be applied in the same way to devices with larger donor–acceptor energetic offsets. In such a case, most of the PL originating from the recombination of free charge carriers will be emitted from CT states. As these states are less emissive compared to LE states, the intensity will be lower. A limitation is imposed by the dynamic range of the detector in the relevant wavelength region, which in our case is about five orders of magnitude.

2.4. Transient PL on Bare Organic Absorber Layers

We have so far demonstrated that the introduced method of transient PL allows the measurement of the free charge carrier luminescence of organic solar cells. We were able to prove this by studying the relation of the measured open-circuit voltage with the calculated implied voltage using complete solar cells with electric contacts.

In addition, the method can also be applied to determine the free charge carrier luminescence of bare absorber layers without electric contacts. This shall be shown in the following. For this, absorber layers of both, PV-X plus and D18:Y6 were deposited on CaF_2 substrates. Transient PL was then performed in the same manner as described above for the complete solar cells. In order to compare the PL of the bare absorber layers with the one of the complete solar cells it is necessary to account for the differing absorption and emission properties of solar cell and bare layer. The ratio of the absorptions $\frac{A_{layer}}{A_{solar\ cell}}$ (0.89 for D18:Y6 and 0.70 for PV-X plus) is used to determine the generation rate. Likewise, the detected luminescence intensities are corrected for the different emission properties $\frac{\alpha_{solar\ cell}}{\alpha_{layer}}$ yielding 2.57 for D18:Y6 and 2.12 for PV-X plus. The detailed calculation of absorption and emission correction is given in the Supporting Information.

Figure 6 depicts the corrected photogenerated LE (blue) as well as the free charge carrier (red) luminescence of the bare absorber layers (closed symbols) alongside the luminescence intensities of the corresponding solar cell (line with open symbols) for A) PV-X plus and B) D18:Y6. The transient PL data and fits of the bare layers are shown in Figure S5 (Supporting Information).

For both organic absorber materials, the LE luminescence intensities of bare layer and solar cell are almost indistinguishable. This indicates that the optical properties have correctly been calculated since the LE luminescence is not expected to depend on the presence/absence of contact layers. The free charge carrier luminescence of both solar cell and bare layer can be calculated to V_{imp} using Equation (6). The implied voltages of bare layers (red stars) and solar cells (grey circles) are plotted alongside V_{OC} (grey line) of the corresponding solar cell in Figure 6c,d. Overall, a very good agreement is observed. Deviations between bare absorber layers and complete solar cells are observed for both absorber materials at low intensities where the implied voltage of the bare absorber layer is larger than V_{OC} and V_{imp} of the complete solar cell. This is most likely a consequence of a finite parallel resistance that limits the voltage severely toward lower intensities.[48] A more detailed analysis is however beyond the scope of this work.

These results clearly demonstrate that the newly developed method to measure the free charge carrier luminescence in organic solar cells can also be successfully applied to bare absorber layers. This enables determining the upper limit for the V_{OC} of a solar cell based on a given absorber material system. It further facilitates the analysis of losses occurring due to the non-ideality of

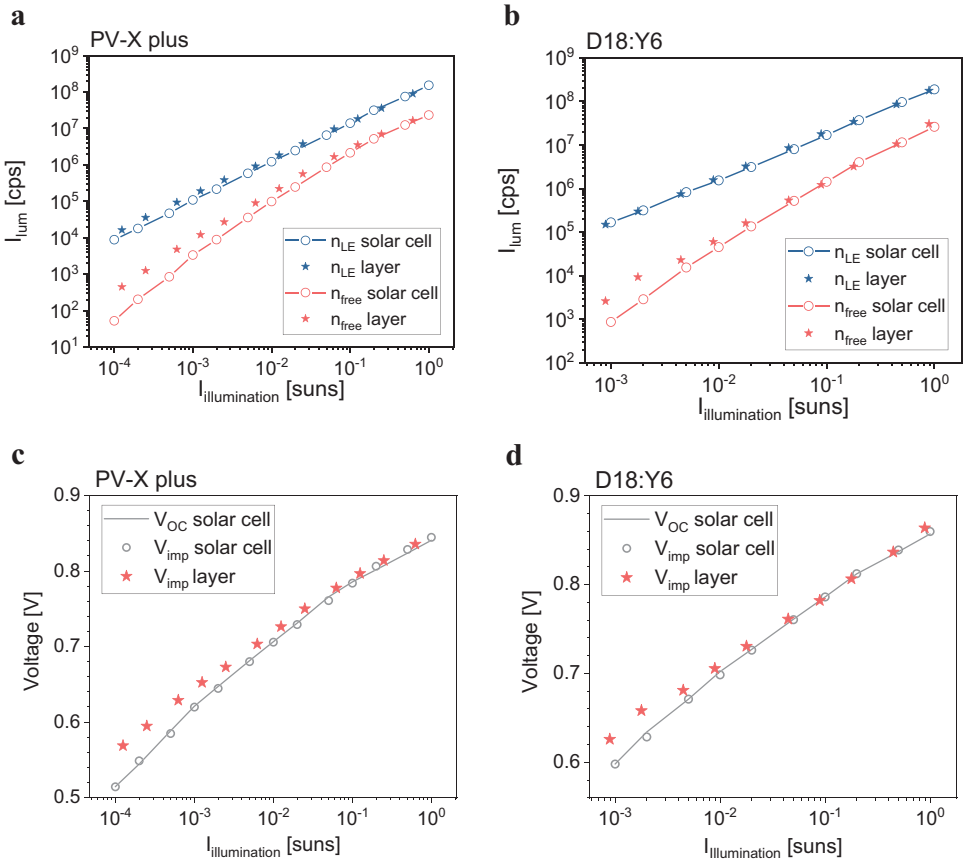

Figure 6. Illumination intensity dependent transient PL of bare absorber layers compared to the one of complete solar cells. The steady-state PL intensity I_{lum} from LE (blue) as well as from free charge carriers (red) for a) a bare PV-X plus and b) a bare D18:Y6 absorber layer together with the PL signals from complete solar cells (line with symbols) for various illumination intensities. Open-circuit voltage (grey line) of complete solar cell and derived implied voltage for solar cell (grey circles) and bare absorber layer (red stars) as a function of illumination intensity for c) PV-X plus and d) D18:Y6.

interfaces between the absorber and the electron and hole transport materials, respectively.

3. Conclusion

In this work, we have introduced a newly developed method to detect the free charge carrier photoluminescence in organic solar cells. In fact, their steady-state PL signal is strongly dominated by photogenerated excitons. The method is therefore based on transient PL measurements and makes use of the fact that the lifetime of photogenerated excitons is much shorter than the one of free electrons and holes. Indeed, our results clearly show, to the best of our knowledge for the first time, that this transient PL method enables disentangling the luminescence stemming from photogenerated excitons from the one originating from free charge carriers. To validate the results the implied voltage (quasi-Fermi level separation divided by elementary charge) was compared to the open-circuit voltage of the investigated organic solar cells. An excellent agreement was found both in steady-state and transient data that proves that we are indeed able to measure the free charge carrier luminescence in organic solar cells. The method further offers the possibility to derive the implied voltage from PL measurements of bare absorber films that was also demonstrated in this work. In summary, this newly developed transient PL method paves the way to take advantage of PL as an important characterization technique also in the field of organic photovoltaics.

4. Experimental Section

Luminescence Measurements: The steady state EL spectra were measured using a Czerny–Turner spectrograph (Andor Shamrock 193i) with an InGaAs photo diode array (Andor iDus DU490A) that was cooled to −50 °C. Transient PL was acquired in a time correlated single photon counting setup as described in detail in the previous work.[45] In addition to transient EL, a 515 nm continuous wave laser with a fall time $t_{off} \approx 1$ ns was used for photoexcitation under an angle of 45°. The laser beam was shaped to a circular spot (diameter ≈1 cm) using a TopHat Converter to illuminate the solar cell homogeneously. On top, a short-passfilter (517 nm) was included at the end of the illumination beam path to suppress any NIR luminescence originating from the optical components. Regarding the beam path of the luminescence, a long-passfilter (532 nm) was placed in front of the detector to block reflected laser light. To minimize external current flow for the time resolved V_{OC} measurement a custom-made high impedance buffer amplifier ($R_{in} > 10^{12}$ Ω) was used in combination with an oscilloscope (picoscope model 5444B). Time-resolved intensity dependent luminescence data was acquired with a time resolution of 20 ns except for the detailed measurement of the decay in Figure 2b where an acquisition with a resolution of 25ps was included. The illumination-time for

transient PL was chosen between 50 µs and 4 ms dependent on the prevalent illumination intensity such that the solar cell reaches steady state. The off-time between two illumination cycles was set to 1ms. The experiment was periodically repeated until at least 50 counts per bin were accumulated during illumination. For high illumination intensities the luminescence was attenuated using neutral density filter to protect the photomultiplier tube. All EL and PL measurements were executed under inert atmosphere. The illumination intensity of "1 sun" was determined by adjusting the laser intensity to generate the same J_{SC} as measured under the solar simulator under "1 sun" (i.e., AM1.5G, corrected for spectral mismatch) and the laser irradiance was measured with a power meter (Thorlabs S121C). This irradiance value was used to recalculate the intensities to units of suns. The laser attenuation was realized by a mechanical aperture.

Solar Cell Preparation: Both solar cells used for the experiments were produced on calcium fluoride substrates (2.5 × 2.5 cm^2) with ITO sputtered on top. The substrates were cleaned in ultrasonic baths of acetone (two times), isopropanol (two times) and finally deionized water, for 5 min each and UV-ozone treated for 20 min. The cell stacks of the used solar cells are: CaF/ITO/PEDOT:PSS/D18:Y6/PDIN/Ag and CaF/ITO/PFN-Br/PV-Xplus/HTL-X/Au/Ag. PEDOT:PSS (Ai4083 from Heraeus) was deposited via spin-coating under air at 3000 rpm and annealed at 130 °C for 10 min under nitrogen. PFN-Br (purchased from Organtec Ltd) was dissolved in methanol (0.5 mg mL^{-1}) and spin coated under nitrogen at 2000 rpm resulting in a layer thickness of ≈5 nm. The absorber materials were deposited via dynamic spin coating under nitrogen. D18:Y6 (purchased from 1-Material) was dissolved in chloroform using a donor:acceptor ratio of 1:1.6 and a concentration of 11 mg mL^{-1}. It was deposited at 2550 rpm yielding a thickness of 120 nm. PV-X plus was mixed using the donor material PV2300 and the acceptor materials PV-A-3 and N1100 (all purchased from Raynergy Tek). The ingredients were dissolved in o-xylene (22 mg mL^{-1}) in a ratio of 1:1:0.2. The solution was spin-coated at 1200 rpm leading to a thickness of 125 nm. PDIN (1-Material) was dissolved in methanol using a concentration of 2 mg mL^{-1}, adding 0.27 vol% acetic acid (p.a. grade from Sigma Aldrich). It was spin coated at 5000 rpm producing a 5 nm thick layer. HTL-X (HTL-XC and HTL-XD mixed in ratio 1:4, both purchased from Raynergy Tek) was spin-coated at 4000 rpm to obtain a thickness of 30 nm and annealed at 110 °C for 10 min under nitrogen. 5nm of gold (for PV-X plus) and 100 nm of silver were deposited via thermal evaporation at a pressure of $< 5 \times 10^{-5}$ mbar.

Supporting Information

Supporting Information is available from the Wiley Online Library or from the author.

Acknowledgements

M.L. and J.F. contributed equally to this work. U.W., M.L., and J.F. acknowledge funding from the German Federal Ministry for Economic Affairs and Climate Protection (FKz. 03EE1119). J.F. acknowledges the scholarship support provided by the German Federal Environmental Foundation (DBU). U.W. thanks Carsten Deibel for the fruitful discussion. The authors thank Leonie Pap for support in optical simulations and Shankar Bogati, Leonard Tutsch, and Vasileios Georgiou-Sarlikiotis for sputtering.

Open access funding enabled and organized by Projekt DEAL.

Conflict of Interest

The authors declare no conflict of interest.

Data Availability Statement

The data that support the findings of this study are available from the corresponding author upon reasonable request.

Keywords

implied voltage, organic solar cells, photoluminescence, quasi-Fermi level separation, radiative recombination

Received: April 15, 2023
Revised: July 19, 2023
Published online:

[1] Y. Cui, Y. Xu, H. Yao, P. Bi, L. Hong, J. Zhang, Y. Zu, T. Zhang, J. Qin, J. Ren, Z. Chen, C. He, X. Hao, Z. Wei, J. Hou, *Adv. Mater.* **2021**, *33*, 2102420.
[2] J. Gao, N. Yu, Z. Chen, Y. Wei, C. Li, T. Liu, X. Gu, J. Zhang, Z. Wei, Z. Tang, X. Hao, F. Zhang, X. Zhang, H. Huang, *Adv. Sci.* **2022**, *9*, 2203606.
[3] W. Gao, F. Qi, Z. Peng, F. R. Lin, K. Jiang, C. Zhong, W. Kaminsky, Z. Guan, C.-S. Lee, T. J. Marks, H. Ade, A. K.-Y. Jen, *Adv. Mater.* **2022**, *34*, 2202089.
[4] Y. Wei, Z. Chen, G. Lu, N. Yu, C. Li, J. Gao, X. Gu, X. Hao, G. Lu, Z. Tang, J. Zhang, Z. Wei, X. Zhang, H. Huang, *Adv. Mater.* **2022**, *34*, 2204718.
[5] L. Hong, H. Yao, Y. Cui, P. Bi, T. Zhang, Y. Cheng, Y. Zu, J. Qin, R. Yu, Z. Ge, J. Hou, *Adv. Mater.* **2021**, *33*, 2103091.
[6] U. Rau, *Phys. Rev. B* **2007**, *76*, 85303.
[7] S. Roensch, R. Hoheisel, F. Dimroth, A. W. Bett, *Appl. Phys. Lett.* **2011**, *98*, 251113.
[8] O. D. Miller, E. Yablonovitch, S. R. Kurtz, *IEEE J. Photovoltaics* **2012**, *2*, 303.
[9] T. Kirchartz, U. Rau, M. Hermle, A. W. Bett, A. Helbig, J. H. Werner, *Appl. Phys. Lett.* **2008**, *92*, 123502.
[10] H. Nesswetter, N. R. Jost, P. Lugli, A. W. Bett, C. G. Zimmermann, *Appl. Phys. Lett.* **2015**, *106*, 23903.
[11] J. Yang, H. W. Du, D. S. Chen, F. Xu, P. H. Zhou, J. Xu, Z. Q. Ma, *Mater. Lett.* **2015**, *145*, 236.
[12] M.-J. Yang, M. Yamaguchi, T. Takamoto, E. Ikeda, H. Kurita, M. Ohmori, *Sol. Energy Mater. Sol. Cells* **1997**, *45*, 331.
[13] A. Delamarre, M. Paire, J.-F. Guillemoles, L. Lombez, *Prog. Photovoltaics: Res. Appl.* **2015**, *23*, 1305.
[14] S. Shirakata, T. Nakada, *Phys. Status Solidi C* **2009**, *6*, 1059.
[15] S. Shirakata, *Phys. Status Solidi B* **2015**, *252*, 1211.
[16] P. Würfel, T. Trupke, T. Puzzer, E. Schäffer, W. Warta, S. W. Glunz, *J. Appl. Phys.* **2007**, *101*, 123110.
[17] T. Trupke, E. Pink, R. A. Bardos, M. D. Abbott, *Appl. Phys. Lett.* **2007**, *90*, 093506.
[18] D. Grecu, A. D. Compaan, D. Young, U. Jayamaha, D. H. Rose, *J. Appl. Phys.* **2000**, *88*, 2490.
[19] D. Kuciauskas, P. Dippo, Z. Zhao, L. Cheng, A. Kanevce, W. K. Metzger, M. Gloeckler, *IEEE J. Photovoltaics* **2016**, *6*, 313.
[20] W. K. Metzger, D. Albin, D. Levi, P. Sheldon, X. Li, B. M. Keyes, R. K. Ahrenkiel, *J. Appl. Phys.* **2003**, *94*, 3549.
[21] O. Nos, W. Favre, F. Jay, F. Ozanne, A. Valla, J. Alvarez, D. Muñoz, P. J. Ribeyron, *Sol. Energy Mater. Sol. Cells* **2016**, *144*, 210.
[22] G. El-Hajje, C. Momblona, L. Gil-Escrig, J. Ávila, T. Guillemot, J.-F. Guillemoles, M. Sessolo, H. J. Bolink, L. Lombez, *Energy Environ. Sci.* **2016**, *9*, 2286.
[23] M. J. Romero, H. Du, G. Teeter, Y. Yan, M. M. Al-Jassim, *Phys. Rev. B* **2011**, *84*, 165324.
[24] T. Kirchartz, J. A. Márquez, M. Stolterfoht, T. Unold, *Adv. Energy Mater.* **2020**, *10*, 1904134.
[25] K. P. Goetz, A. D. Taylor, F. Paulus, Y. Vaynzof, *Adv. Funct. Mater.* **2020**, *30*, 1910004.
[26] A. Dkhissi, *Synth. Met.* **2011**, *161*, 1441.

[27] P. Puschnig, C. Ambrosch-Draxl, *C. R. Phys.* **2009**, *10*, 504.
[28] H.-W. Li, Z. Guan, Y. Cheng, T. Lui, Q. Yang, C.-S. Lee, S. Chen, S.-W. Tsang, *Adv. Electron. Mater.* **2016**, *2*, 1600200.
[29] M. Knupfer, *Appl. Phys. A* **2003**, *77*, 623.
[30] J.-L. Bredas, J. E. Norton, J. Cornil, V. Coropceanu, *Acc. Chem. Res.* **2009**, *42*, 1691.
[31] M. List, T. Sarkar, P. Perkhun, J. Ackermann, C. Luo, U. Würfel, *Nat. Commun.* **2018**, *9*, 3631.
[32] Q. Liu, Y. Jiang, K. Jin, J. Qin, J. Xu, W. Li, J. Xiong, J. Liu, Z. Xiao, K. Sun, S. Yang, X. Zhang, L. Ding, *Sci. Bull.* **2020**, *65*, 272.
[33] A. Spies, M. List, T. Sarkar, U. Würfel, *Adv. Energy Mater.* **2017**, *7*, 1601750.
[34] D. B. Riley, O. J. Sandberg, N. M. Wilson, W. Li, S. Zeiske, N. Zarrabi, P. Meredith, R. Österbacka, A. Armin, *Phys. Rev. Appl.* **2021**, *15*, 64035.
[35] Q. L. Phuong, S. M. Hosseini, O. J. Sandberg, Y. Zou, H. Y. Woo, D. Neher, S. Shoaee, *Sol. RRL* **2021**, *5*, 2000649.
[36] S. D. Dimitrov, B. C. Schroeder, C. B. Nielsen, H. Bronstein, Z. Fei, I. McCulloch, M. Heeney, J. R. Durrant, *Polymers* **2016**, *8*, 14.
[37] A. P. Arndt, M. Gerhard, A. Quintilla, I. A. Howard, M. Koch, U. Lemmer, *J. Phys. Chem. C* **2015**, *119*, 13516.
[38] A. Classen, C. L. Chochos, L. Lüer, V. G. Gregoriou, J. Wortmann, A. Osvet, K. Forberich, I. McCulloch, T. Heumüller, C. J. Brabec, *Nat. Energy* **2020**, *5*, 711.
[39] K. Vandewal, *Annu. Rev. Phys. Chem.* **2016**, *67*, 113.
[40] T. M. Clarke, J. R. Durrant, *Chem. Rev.* **2010**, *110*, 6736.
[41] M. Azzouzi, P. Calado, A. M. Telford, F. Eisner, X. Hou, T. Kirchartz, P. R. F. Barnes, J. Nelson, *Sol. RRL* **2020**, *4*, 1900581.
[42] G. Garcia-Belmonte, P. P. Boix, J. Bisquert, M. Sessolo, H. J. Bolink, *Sol. Energy Mater. Sol. Cells* **2010**, *94*, 366.
[43] J. Wu, H. Cha, T. Du, Y. Dong, W. Xu, C.-T. Lin, J. R. Durrant, *Adv. Mater.* **2022**, *34*, 2101833.
[44] Y. He, B. Wang, L. Lüer, G. Feng, A. Osvet, T. Heumüller, C. Liu, W. Li, D. M. Guldi, N. Li, C. J. Brabec, *Adv. Energy Mater.* **2022**, *12*, 2103406.
[45] J. Faisst, M. List, F. Heinz, U. Würfel, *Adv. Opt. Mater.* **2022**, *10*, 2200909.
[46] F. D. Eisner, M. Azzouzi, Z. Fei, X. Hou, T. D. Anthopoulos, T. J. S. Dennis, M. Heeney, J. Nelson, *J. Am. Chem. Soc.* **2019**, *141*, 6362.
[47] J. Hofinger, C. Putz, F. Mayr, K. Gugujonovic, D. Wielend, M. C. Scharber, *Mater. Adv.* **2021**, *2*, 4291.
[48] D. Müller, L. Campos Guzmán, E. Jiang, B. Zimmermann, U. Würfel, *Sol. RRL* **2022**, *6*, 2200175.